ELSEVIER

Layered double hydroxides as potential chromate scavengers

Srinivasa V. Prasanna, R. Anantha Padmanabha Rao, P. Vishnu Kamath [*]

Department of Chemistry, Central College, Bangalore University, Bangalore 560001, India

Received 31 July 2006; accepted 31 August 2006

Available online 5 October 2006

Abstract

The LDH of Ni with Fe, having the formula $Ni_{1-x}Fe_x(OH)_2(A^{n-})_{x/n} \cdot yH_2O$ (A = NO_3^-, Cl^-; x = 0.25, 0.33), scavenges CrO_4^{2-} ions from solution throughout the concentration range examined (0.00625–0.25 N). The CrO_4^{2-} uptake capacity is independent of the anion in the starting LDH but is higher when x = 0.25 (3.60 meq g^{-1}) as compared to x = 0.33 (2.40 meq g^{-1}). These values are higher than those observed for control compounds β-$Ni(OH)_2$ (1.86 meq g^{-1}) and FeO(OH) (1.26 meq g^{-1}), which do not have any interlayer chemistry, showing that chromate uptake takes place by its incorporation in the interlayer region by a stoichiometric anion-exchange reaction, rather than by adsorption. Nevertheless, the interaction between the LDH and the chromate ions is weak. The weak interaction is due to the mismatch between the symmetry of the chromate ions and the symmetry of the interlayer site, which introduces turbostratic disorder in the chromate-intercalated LDHs. The chromate ions can be completely leached out by soaking the LDH in a sodium carbonate solution.

© 2006 Elsevier Inc. All rights reserved.

Keywords: Layered double hydroxides; Chromate uptake; Anion exchange

1. Introduction

Common methods employed to remediate insidious anions such as chromate, arsenate, phosphates, and iodides from waste waters include (i) adsorption using materials with chemically active sites and porous physical structure [1,2], (ii) precipitation [3], (iii) coprecipitation [4], and (iv) ion exchange [5]. Of the various methods, ion exchange confers on the solid the highest capacity for the contaminant. The solids which are currently widely used comprise two structure types:

(a) Those such as silica and activated alumina that have a three-dimensional structure and are therefore active only by adsorption. This is a surface phenomenon where the bulk of the solid is not used for remediation.

(b) Solids such as $Mg(OH)_2$, $Al(OH)_3$, ferrihydrite, goethite, and boehmite [4] have a layered structure that enhances the interfacial surface area. However, these solids comprise charge-neutral layers and hence have no interlayer chemistry.

The layered double hydroxides (LDHs) are related to the latter class of compounds. Structurally and functionally they are the inverse of the better-known smectite-type cationic clays [6]. While cationic clays have negatively charged aluminosilicate or magnesiosilicate layers [7], the LDHs are made up of positively charged layers having the composition $[M_{1-x}^{II}M_x'^{III}(OH)_2]^{x+}$ (M = Mg, Ca, Ni, Co, Cu, Zn; M' = Al, V, Cr, Fe, Ga, In; $0.15 \leqslant x \leqslant 0.33$) [8]. Anions are incorporated between the layers to restore charge neutrality in much the same way that alkali and alkaline earth metal cations are intercalated in cationic clays. The resulting compounds have the formula $[M_{1-x}^{II}M_x'^{III}(OH)_2]^{x+}(A^{n-})_{x/n} \cdot yH_2O$. We refer to these LDHs as M–M'–A^{n-}.

The LDHs exhibit properties such as anionic mobility [9] and surface basicity [10]. The LDHs also participate in anion-exchange reactions and incorporate a wide variety of anions, such as inorganic anions, oxometallates, carboxylates, phosphates and phosphonates, sulfates and sulfonates, amino acids, peptides, and nucleotides. The complete range of exchange reactions and the resulting inorganic–organic hybrid compounds have been extensively reviewed [11–13]. As an extension of these properties, LDHs have been identified as potential sinks for hazardous anionic contaminants in industrial and waste wa-

---

ter systems. Cr(VI) in the forms CrO_4^{2-} and $Cr_2O_7^{2-}$ is among the more insidious anionic contaminants in wastewater and the Mg–Al LDH has been employed for chromate sorption from aqueous solutions [14]. Chromate sorption from dilute solutions (15–30 ppm) by Zn–Al LDH has also been reported [15].

However, the utility of LDHs in immobilization of anionic waste by exchange reactions suffers from severe limitations.

(1) LDHs have a special affinity for carbonate ions and incorporate carbonates from CO_2 present in the ambient. The carbonate-containing LDHs are also the most stable in comparison to LDHs with other anions [16]. Therefore CO_3^{2-}-containing LDHs do not participate in any exchange reactions and are ineffective in scavenging anionic contaminants. CO_2 has to be rigorously excluded from exchange reactions, thus severely limiting the widespread use of LDHs in the ambient.

(2) Generally Cl^- and NO_3^--containing LDHs are used for anion sorption, and these are released into the environment. Cl^- and NO_3^- ions are themselves considered environmental hazards.

(3) As exchange reactions are activity-driven, the concentration of the incoming anion is maintained at two to five times the stoichiometric requirement in the reaction medium [17,18]. In water purification applications, often the anionic pollutant is present at very low concentration.

(4) The LDHs have substantial solubility in water [16], and many authors report bulk mass loss during anion exchange [19–21]. In this case the LDHs themselves are sources of heavy metals. This severely restricts the choice of LDHs to those containing benign cations such as Mg^{2+}, Ca^{2+}, Al^{3+}, and Fe^{3+}. The LDH solubility is driven by the solubility of the salt of the divalent ion [16] and therefore LDHs of Ca^{2+} and Mg^{2+} with their higher solubilities, compared to those of transition-metal-cation-containing LDHs, tend to be less efficient in scavenging anions. Thus, the Mg–Fe–NO_3^- LDH fails to scavenge chromate ions [22].

(5) There is evidence that the anion-exchange reactions take place by dissolution reprecipitation rather than topotactically [23]. Therefore unless the LDH composing the incoming ion is more insoluble than the original LDH, exchange reactions are unlikely to take place.

In light of all these issues, there is an urgent need to investigate the anion uptake characteristics of a model LDH system. We have chosen the Ni–Fe LDH as a model, as it has a low solubility product ($pK_{sp} = 60.81$) [24] compared to other LDHs, by which extraneous factors arising from the solution chemistry of the LDHs are mitigated.

2. Experimental

2.1. Synthesis of LDHs

All reagents were of analytical grade (Merck, India) and were used without further purification. The M–M′–X (X = Cl^-,

NO_3^-) LDHs were prepared by drop-wise addition (3 ml min^{-1}) of a mixed salt solution ($MX_2 + M'X_3$) into a reservoir containing 10 times the stoichiometric requirement of X^- ions taken as its sodium salt. A 2 N NaOH solution was dispensed using a Metrohm Model 718 STAT Titrino to maintain a constant pH at precipitation (pH 7). N_2 gas was bubbled through the solution during precipitation and aging for 18 h at 65 °C. The precipitate was rapidly filtered under suction, washed with deionized (10^{15} Ω cm specific resistance), decarbonated water, and then dried at 80 °C for 24 h. The Ni–Fe LDHs were also hydrothermally treated in a Teflon-lined autoclave (150 ml, 50% filling) under autogenous pressure at 140–160 °C for 18 h to facilitate crystal growth. The Ni–Fe–CO_3^{2-} LDH was prepared by the method of Reichle [25] at a constant high pH > 11 and worked up as above. The Ni/Fe ratio was varied from 3 to 2 corresponding to x values of 0.25 and 0.33, respectively. β-Ni(OH)$_2$ and FeO(OH) were prepared by standard methods reported in the literature and used as controls [26].

2.2. Characterization

All samples were characterized by powder X-ray diffraction using an X'pert Pro Philips diffractometer (Cu$K\alpha$ source, $\lambda = 1.541$ Å) fitted with a graphite monochromator. IR spectra were recorded using a Nicolet Model Impact 400D FTIR spectrometer (4000–400 cm^{-1}, resolution 4 cm^{-1}, KBr pellet). The surface areas of the samples were measured using a NOVA 1000 Version 3.70 high-speed gas sorption analyzer. Wet chemical analysis for CrO_4^{2-} was done by dissolving a preweighed (0.2 g) quantity of the sample in acid (2 ml conc. H_2SO_4) and titrating against standard ferrous ammonium sulfate (0.025 N) potentiometrically.

2.3. Chromate uptake studies

Preweighed (0.20 g) batches of the LDH were suspended in 25 ml of decarbonated water and stirred for 30 min to ensure complete wetting. To this slurry 25 ml of K_2CrO_4 solution (0.0125–0.25 N, pH 8.2) was added and stirred for 5 h at the ambient temperature (23–25 °C), after which the slurry was centrifuged and the chromate concentration of the centrifugate determined by means of potentiometric titration versus standard (0.025–0.1 N) ferrous ammonium sulfate (FAS) solution. For low chromate concentrations ($\leqslant$0.00625 N), a larger volume (50–100 ml) of the K_2CrO_4 solution was used to effect the chromate uptake. Chromate uptake was also measured from K_2CrO_4 solutions, which were made 1 N in the potassium salt of the outgoing ion. In this manner, the concentration of the outgoing ion was maintained nearly constant to study the effect of relative activities of the anions on the uptake of chromate ions. The chromate uptake by the LDHs was calculated from the difference in the initial and final chromate concentrations and is reported in milliequivalents per gram of the LDH taken. From this data, isotherms were plotted.

In the case of the Ni–Fe–CO_3^{2-} LDH, the suspension was first titrated versus an HCl solution (0.05 N) containing the stoichiometric requirement of acid required to decompose the inter-

calated carbonate. The pH during the titration was maintained at 4.5. This titration is expected to yield the chloride-containing LDH. Chromate solution was then added and the mixture stirred at ambient temperature (23–25 °C) for 5 h. The pH was maintained at 4.5 throughout the reaction to exclude CO_2.

Conventional anion-exchange reactions were carried out by suspending preweighed (0.25 g) batches of the LDH in 30 ml of K_2CrO_4 solution containing 10 times the stoichiometric requirement of chromate ions to effect complete exchange of the anions in the starting LDH. The reaction was carried out for 5 h with stirring, after which the solid was separated by centrifugation and washed with deionized, decarbonated water. The chromate uptake observed in these experiments is referred to as the "chromate exchange capacity" and is compared with the theoretical exchange capacity computed from the molecular formula.

3. DIFFaX studies

The nature of structural disorder in the LDHs was studied by simulation of the PXRD patterns using the FORTRAN-based computer program DIFFaX [27]. The details of DIFFaX simulations of LDHs are described in our earlier papers [28,29]. In this paper, the structure of the Zn–Al–Cl⁻ LDH (ICSD No. 91155, space group R-$3m$, $a = 3.0842$ Å, $c = 23.4706$ Å) is used as the model to describe the layer. Turbostratic disorder was introduced by stacking the metal hydroxide layers using the vector $(x, y, 1/3)$ (x, y are random numbers). Within the DIFFaX formalism, the particle size is described in terms of the disc diameter and thickness. The former is a measure of the crystallite size in the a–b plane and the latter defines the number of layers stacked along the c crystallographic axis. Restricting particle thickness selectively broadens the basal reflections, whereas a small disc diameter broadens all reflections. The broadening is nonuniform, with the $hk0$ being affected the most. The thickness value was varied systematically till a good visual fit was obtained between the calculated and observed PXRD patterns in the 2θ range 10°–25° which contains the basal reflections. A good fit in the high-angle (>25° 2θ) region was obtained by the inclusion of turbostratic disorder.

4. Results and discussion

In Fig. 1 is shown the chromate uptake by the Ni–Fe–NO_3^- ($x = 0.25$) LDH at different initial chromate concentrations. At each concentration, sufficient volume of the K_2CrO_4 solution was fed to achieve maximum uptake. The saturation uptake increases with the initial concentration and reaches a maximum at an initial concentration of 0.2 N. The maximum uptake (3.60 meq g⁻¹) agrees with the chromate exchange capacity obtained from a conventional exchange reaction. This value is higher than the cation carrying capacity of smectite-type clays, which is typically 0.87 meq g⁻¹ [7]. Clearly the large chromate uptake involves the incorporation of chromate ions into the interlayer region.
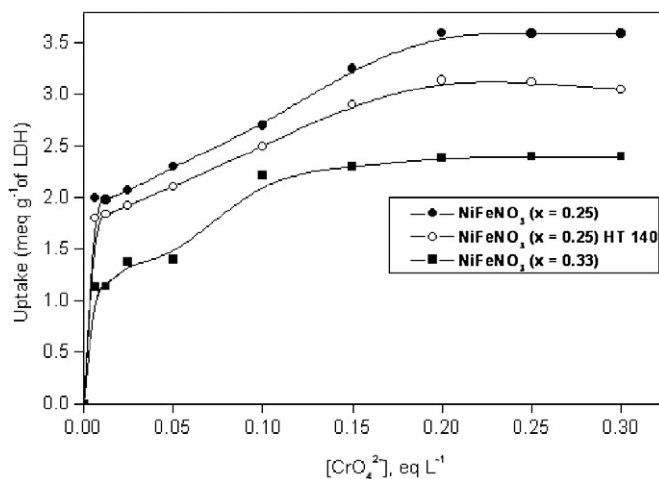

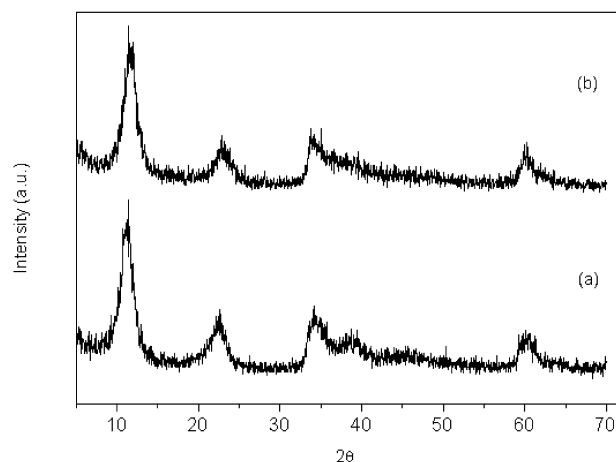Fig. 1. Chromate uptake isotherms of Ni–Fe–NO_3^- LDHs.

Fig. 2. Powder X-ray diffraction patterns of the Ni–Fe–NO_3^- ($x = 0.25$) LDH (a) before and (b) after chromate exchange.

4.1. Powder X-ray diffraction (PXRD) studies

The PXRD patterns of the LDH and the product obtained after chromate exchange are shown in Fig. 2. The starting material exhibits all the reflections expected of the LDH. The low-angle reflection appearing at 11.1° 2θ ($d = 8.0$ Å) corresponds to the interlayer spacing. Its higher harmonic appears at 22.6° 2θ ($d = 4.0$ Å). In the mid-2θ (30°–50°) region a broad peak with a sawtooth lineshape is observed. This is attributed to structural disorder [29] arising out of stacking faults and therefore no attempt is made here to index it. At high angles, a single broad band composed of the 110 and 113 reflections is observed. The LDH can be indexed to a hexagonal cell ($a = 2d_{110} = 3.068$ Å; $c = 8.0$ Å). These features are essentially retained after chromate exchange (see Fig. 2b) except for a slight broadening of the peaks. This enhanced broadening is on account of the tetrahedral symmetry of the CrO_4^{2-} ion. The sites available in the interlayer region of the LDHs are compatible to anions having D_{3h} symmetry [30]. When anions having other symmetries enter the interlayer region, the registry between successive layers is lost, resulting in what is known as turbostratic disorder [31]. The random orientation of
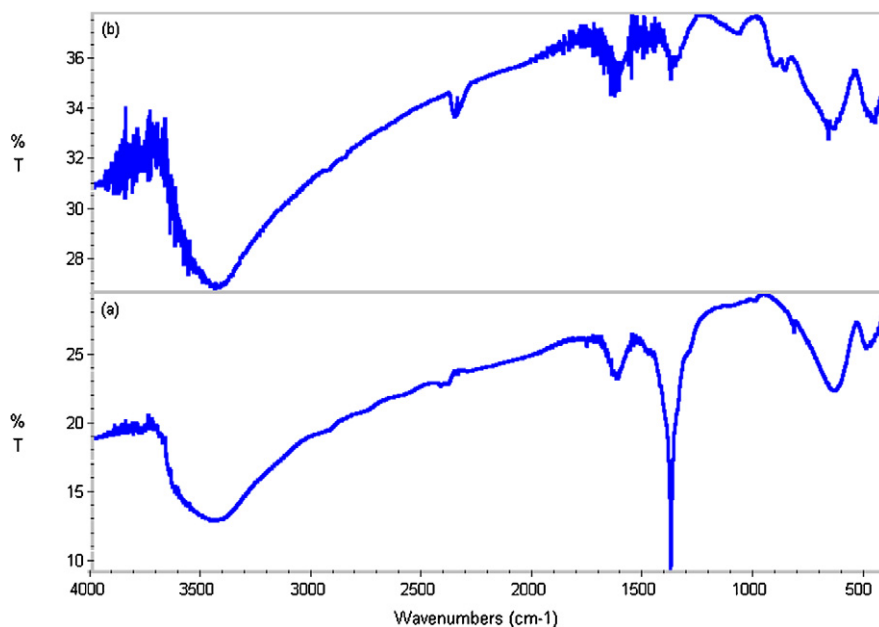
Fig. 3. IR spectrum of the Ni–Fe–NO_3^- LDH (a) before and (b) after chromate exchange.
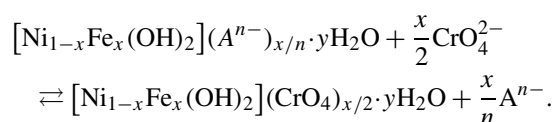
the layers about the c-crystallographic axis results in the sawtooth lineshape of the $hk0$ reflections [29]. Incorporation of CrO_4^{2-} ions does not affect the interlayer spacing as reported elsewhere [32].

4.2. IR spectroscopy

Evidence for chromate incorporation can be found in the IR spectra (see Fig. 3). The starting compound exhibits strong absorption due to the interlayer nitrate at 1383 cm^{-1}, while after the sorption experiment, the nitrate absorption has gone down in intensity and absorption due to intercalated CrO_4^{2-} can be seen at 866 and 917 cm^{-1}. The tetrahedral chromate ion has only two IR-active modes, namely, the antisymmetric stretch (ν_3) and the symmetric deformation mode (ν_4). The latter is expected to appear at 330 cm^{-1}. The observed features are therefore due to the triply degenerate (F_2) ν_3 mode of the chromate. Using Halford's rules, the c-crystallographic axis is treated as the main axis of symmetry of the intercalated chromate, so that the latter behaves as if it belonged to the C_{3v} symmetry [33]. In this lower symmetry, the antisymmetric stretching vibration splits into two modes (A_1 + E). The symmetry is lowered due to grafting, hydrogen bonding, and other interactions with the hydroxide layer [34].

4.3. Chromate uptake studies

The anion exchange reaction takes place according to the equation

$$\left[Ni_{1-x}Fe_x(OH)_2\right](A^{n-})_{x/n}\cdot yH_2O + \frac{x}{2}CrO_4^{2-}$$
$$\rightleftharpoons \left[Ni_{1-x}Fe_x(OH)_2\right](CrO_4)_{x/2}\cdot yH_2O + \frac{x}{n}A^{n-}.$$

The chromate exchange capacity would then depend upon (i) the positive charge on the hydroxide layer, x; (ii) the leaving

tendency of the outgoing ion, A^{n-}; and (iii) the thermodynamic stability of the CrO_4^{2-}-containing LDH.

4.3.1. Effect of layer charge
Two aspects limit the maximum positive charge on the hydroxide layer.

(1) In the LDH structure, all cations occupy octahedral sites. No two neighboring sites can afford to accommodate trivalent ions because of the large cation–cation repulsion. Thus isotypic trivalent hydroxides such as $Al(OH)_3$ have one-third of cation sites vacant in each metal–hydroxide slab, and where such vacancies are not permitted, some of the hydroxide ions turn into oxides to yield compounds of the type MO(OH) (M = Mn, Co, Ni) [35]. None of these have any interlayer chemistry. Among the LDHs the value of x is limited to the range $0.2 \leqslant x \leqslant 0.33$ [8].
(2) The number of interlayer sites is fixed and amounts to 1 site per cation. This site is shared between the oxygen atoms of the anion and intercalated water [30]. The number of crystallographically defined interlayer sites in a carbonate-containing LDH is limited to C_xO, where $(3x)O$ atoms belong to carbonate and $(1 − 3x)$ belong to the intercalated water [30]. Therefore the positive charge on the layer is also limited by the packing of anions in the interlayer. Naturally occurring LDHs have $x = 0.25$ and 0.33.

To determine the dependence of the CrO_4^{2-} carrying capacity on x, Ni–Fe–NO_3^- LDH with $x = 0.33$ was also prepared. The CrO_4^{2-} uptake and the chromate exchange capacity of the Ni–Fe–NO_3^- ($x = 0.33$) was found to be only 2.40 meq g^{-1}, lower than its $x = 0.25$ counterpart (see Fig. 1). The lower capacity of the LDH with a higher x value is on account of the higher electrostatic attraction between the A^{n-} species and the metal
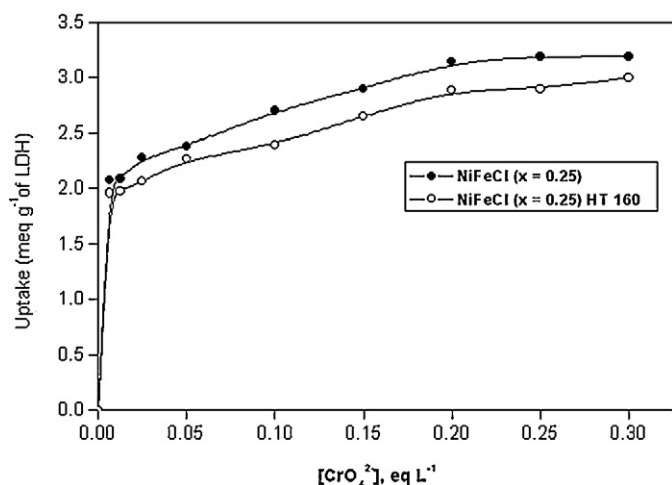
Fig. 4. Chromate uptake isotherms of Ni–Fe–Cl⁻ LDHs.

hydroxide slab. This makes the A^{n-} species a poorer leaving group when the x value is large. Among the cationic clays, too, the micas with high negative charge do not participate in ion-exchange reactions.

4.3.2. Effect of leaving group

To study the effect of the leaving group, chromate uptake studies were carried out with the Cl⁻-containing Ni–Fe LDH ($x = 0.25$) (see Fig. 4). The maximum chromate uptake equals the chromate exchange capacity and was found to be 3.19 meq g⁻¹. Although this value is apparently lower than that of the NO_3^--containing LDH (3.60 meq g⁻¹), the capacity computed as mmole of chromate per mole of the LDH is 0.12 for the Cl⁻-LDH and 0.14 for the NO_3^--LDH, while expected theoretical capacity is 0.125. The higher than theoretical value for the nitrate-LDH is attributed to formation of binary chromates. The two anions therefore have comparable leaving tendency, indicating that the leaving tendency is determined by the charge on the anion rather than the size.

4.3.3. Effect of anion charge

To examine the effect of the charge on the anion, the chromate uptake by Ni–Fe–CO_3^{2-} ($x = 0.25$) LDH was studied. It did not exhibit any chromate uptake, showing CO_3^{2-} to be a poor leaving group. There are two reasons for this.

(i) Higher valent ions in general have a poor leaving tendency, owing to the stronger electrostatic forces of attraction to the host lattice. Even in the case of cationic clays, the monovalent cations are readily replaced by the divalent cations, but not vice versa.

(ii) The LDHs generate prismatic interlayer sites [36], which accommodate CO_3^{2-} ions with their planes parallel to the layers. Such a mode of incorporation maximizes the H-bonding interactions between the carbonate moieties and the protons on the hydroxyl groups. Removal of carbonate ions therefore involves the loss of a significant amount of hydrogen bonding and the corresponding enthalpy. In contrast, nitrate ions bind with their planes perpendicular to the hydroxide layers.

Therefore the carbonates have to be first discharged by reaction with a mineral acid (HCl) in order to facilitate chromate uptake. CO_3^{2-} ions were decomposed under pH stat conditions at pH 4.5. The resultant chromate carrying capacity is 5.79 meq g⁻¹, which is much higher that the theoretically expected value (3.45 meq g⁻¹). This is due to the formation of binary compounds. During the discharge of the intercalated carbonate ions from the LDH by acidification, there is considerable bulk dissolution followed by precipitation of binary nickel chromate. The PXRD pattern of the exchanged sample in the case of Ni–Fe–CO_3^{2-} (data not shown) is poor, showing a high degree of disorder and pointing to the presence of binary compounds with poor crystallinity.

The chromate uptake by the LDHs at different concentrations is listed in Table 1.

4.3.4. Surface contributions to uptake

The chromate carrying capacity of a LDH is expected to arise due to (i) adsorption of CrO_4^{2-} onto the surface of the LDH particles and (ii) CrO_4^{2-} incorporation in the interlayer region by anion exchange. To estimate the former, sorption studies were carried out on two related compounds, β-Ni(OH)₂ and FeO(OH). Both these compounds comprise charge-neutral layers and they do not posses any interlayer chemistry. They were found to have a sorption capacity of 1.86 and 1.26 meq g⁻¹, respectively. These values reflect the contribution of the surface. The higher values observed among the LDHs are clearly due to chromate incorporation into the interlayer region of the bulk.

Table 1
Results of chromate uptake studies on different LDHs

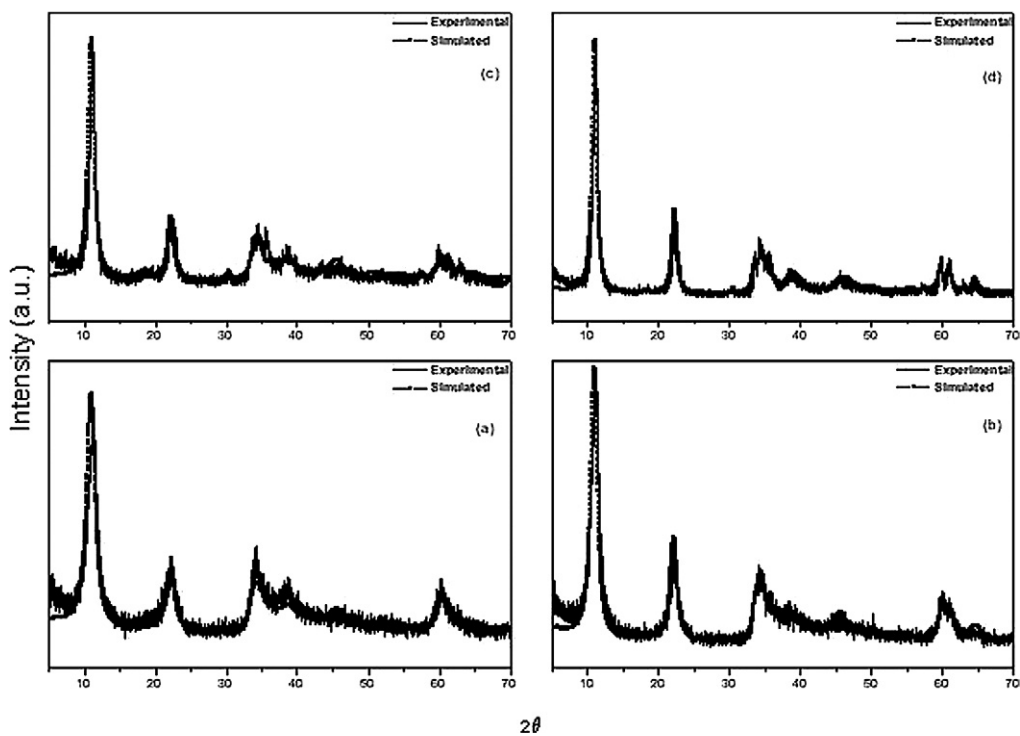| Concentration of K_2CrO_4 (N)	Ni–Fe–NO_3^- ($x = 0.25$) (meq g⁻¹)	Ni–Fe–NO_3^- ($x = 0.25$) HT 140 °C (meq g⁻¹)	Ni–Fe–NO_3^- ($x = 0.33$) (meq g⁻¹)	Ni–Fe–Cl⁻ ($x = 0.25$) (meq g⁻¹)	Ni–Fe–Cl⁻ ($x = 0.25$) HT160 °C (meq g⁻¹)	Ni–Fe–CO_3^{2-} ($x = 0.25$) (meq g⁻¹)
0.00625	2.00	1.80	1.13	2.08	1.96	1.08
0.0125	1.98	1.84	1.14	2.09	1.98	1.40
0.025	2.07	1.93	1.38	2.28	2.07	1.92
0.05	2.30	2.11	1.40	2.38	2.27	3.24
0.10	2.70	2.50	2.22	2.70	2.39	3.66
0.15	3.25	2.90	2.30	2.90	2.65	4.00
0.20	3.60	3.14	2.39	3.14	2.89	4.91
0.25	3.59	3.12	2.40	3.19	2.90	5.79
0.30	3.59	3.05	2.40	3.19	3.00	*

Note. HT: hydrothermally treated.

Fig. 5. Powder X-ray diffraction patterns of the pristine (a, b) and hydrothermally treated (c, d) LDHs. (a, c) Ni–Fe–Cl$^-$ ($x = 0.25$) LDH; (b, d) Ni–Fe–NO$_3^-$ ($x = 0.25$) LDH. The DIFFaX simulations are also shown.
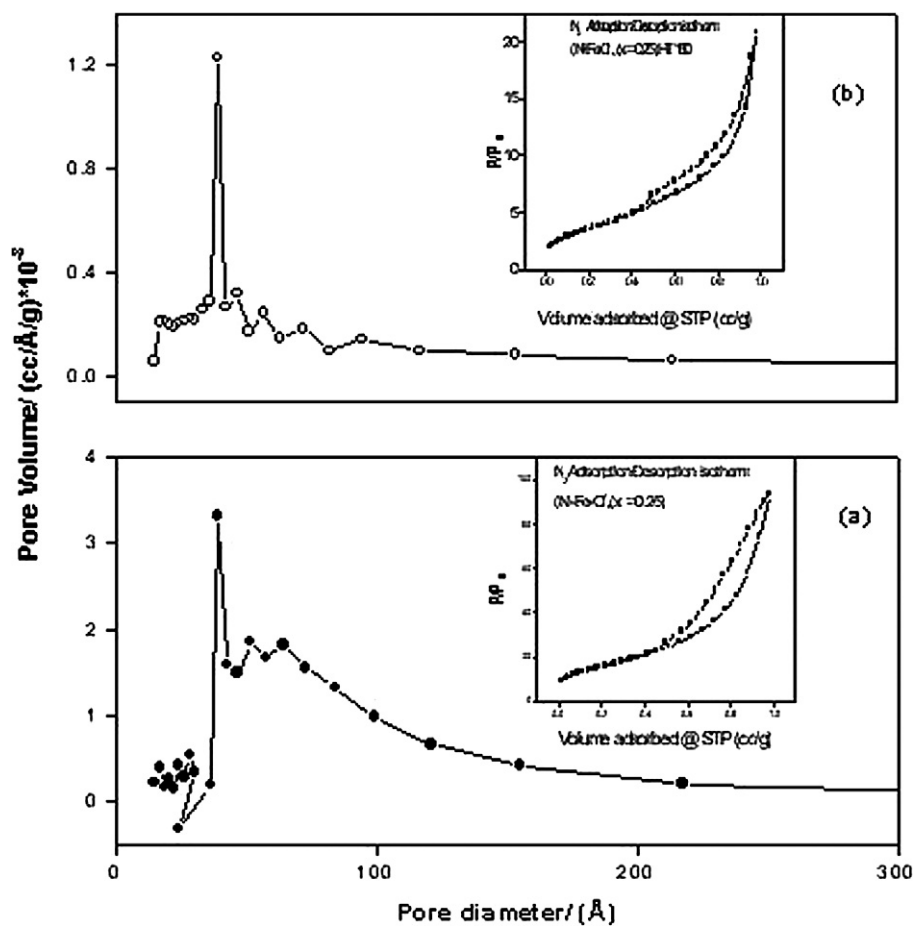

Fig. 6. Pore size distribution in the (a) pristine and (b) hydrothermally treated Ni–Fe–Cl$^-$ ($x = 0.25$) LDH. Inset shows the N$_2$ adsorption–desorption isotherms.

The surface contribution is dependent on the surface area of the sample, while the bulk contribution is expected to be independent of the surface area, especially given the high diffusion coefficients of anions in the LDHs [9].

4.3.5. Effect of surface area

To examine the effect of surface area on chromate uptake, the LDHs were hydrothermally treated. The chromate uptake by the hydrothermally treated LDHs is given in Figs. 1 and 4. Hydrothermal treatment promotes crystal growth and this manifests in the sharper reflections observed in the PXRD pattern of the hydrothermally treated sample. In Fig. 5 are shown the PXRD patterns of the Ni–Fe–X LDHs (X = Cl$^-$, NO$_3^-$) before and after hydrothermal treatment. Also shown are the DIFFaX simulations incorporating the effects of particle size and turbostratic disorder. In Fig. 6 are shown the results of illustrative BET measurements performed on the Ni–Fe–Cl$^-$ LDH. The particle size estimated from DIFFaX simulations and the specific surface areas obtained from BET studies for all the LDHs are given in Table 2. It is clear that on hydrothermal treatment there is a 200–300% increase in particle size while the specific surface area falls to 10–20% of the original value. In Table 2 are also given the chromate exchange capacities of all the LDHs. The chromate uptake capacity declined marginally by about 6–12%, showing that chromate uptake is more in the interlayer, adsorption on the crystallite surface making only a minor contribution. It is evident that the chromate uptake is independent of particle size as the interlayer region is a characteristic of crystal structure and independent of the morphological attributes.

4.4. Nature of chromate uptake

The question now arises as to the nature of the chromate uptake process. The chromate uptake data in Figs. 1 and 4 have the characteristics of a Langmuir isotherm. Many authors have treated the anion uptake process by LDHs within the limits of Langmuir adsorption [37]. This is not strictly correct, as the Langmuir adsorption process is valid only when [38]

 (i) the active sites are empty or
(ii) the outgoing ion is present in sufficient excess for its concentration to be treated as constant.

In the case of the LDHs, the sites of chromate sorption are previously occupied by NO$_3^-$ or Cl$^-$ ions. Therefore chromate
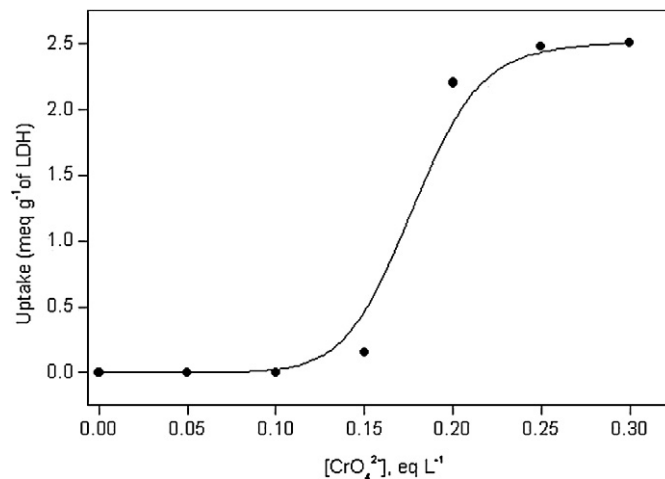

Fig. 7. Chromate uptake isotherm of the Ni–Fe–NO$_3^-$ ($x = 0.25$) LDH in the presence of excess dissolved KNO$_3$.

uptake by the Ni–Fe–NO$_3^-$ ($x = 0.25$) LDH was also studied in the presence of a large excess (1 M) of NaNO$_3$. The results are shown in Fig. 7. It is clear that at low concentrations, there is no uptake, and chromate uptake begins only at an initial concentration of 0.15 N. The resulting isotherm is of Type V, which is typical of a weak adsorbate–adsorbent interaction, chromate uptake being the result of cooperative forces, once some initial uptake has taken place. Subsequent to the initial uptake, the bonding of nitrate ions in the neighborhood of chromate ions weakens, facilitating further uptake of chromate ions.

The weak interaction of chromate with the LDH is understandable from a crystallographic view, as the chromate ion symmetry is incompatible with that of the interlayer site. This results in turbostratic disorder, making the chromate–LDH thermodynamically unstable. The instability of the chromate–LDH is evident when the LDHs are dispersed in Na$_2$CO$_3$ solution (see Table 2). The leaching studies indicated that chromate could be fully leached out by the CO$_3^{2-}$ ions. This is understandable given the thermodynamic stability of carbonate-containing LDHs [16].

5. Conclusion

In conclusion, the use of LDHs for water purification by amelioration of anionic contaminants is fraught with many limitations, mainly arising from the solubility of LDHs. The Ni–Fe LDH chosen as a model system efficiently sorbs chromates

Table 2
Comparison of the specific surface areas and chromate exchange capacities of the LDHs before and after hydrothermal treatment

LDH ($x = 0.25$)	Specific surface area (m^2 g^{-1})	Crystallite size from DIFFaX simulations (Å)	Chromate exchange capacity (meq g^{-1})	CrO$_4^{2-}$ leaching (meq g^{-1})
Ni–Fe–NO$_3^-$	71.23	112	3.60	3.44
Ni–Fe–NO$_3^-$ HT 140 °C	5.03	280	3.14	3.09
Ni–Fe–Cl$^-$	56.65	96	3.19	3.24
Ni–Fe–Cl$^-$ HT 160 °C	13.27	288	3.00	2.91

Note. HT: hydrothermally treated.

ions from solution over a wide concentration range (0.00625–0.30 N) by an anion-exchange reaction, leading to chromate incorporation into the interlayer region. The resulting chromate-containing solid is turbostratically disordered and thermodynamically unstable.

Acknowledgments

References

[1] V.K. Gupta, I. Ali, J. Colloid Interface Sci. 271 (2004) 321.
[2] V.K. Gupta, S. Sharma, Environ. Sci. Technol. 36 (2002) 3612.
[3] A. Lu, S. Zhong, J. Chen, J. Shi, J. Tang, X. Lu, Environ. Sci. Technol. 40 (2006) 3064.
[4] W.R. Richmond, M. Loan, J. Morton, G.M. Parkinson, Environ. Sci. Technol. 38 (2004) 2368.
[5] H. Zhao, K.L. Nagy, J. Colloid Interface Sci. 274 (2004) 613.
[6] F. Trifiro, V. Vaccari, in: G. Alberti, T. Bein (Eds.), Comprehensive Supramolecular Chemistry, vol. 7, Pergamon, Oxford, 1997, p. 251, ch. 8.
[7] T.J. Pinnavaia, Science 220 (1983) 365.
[8] F. Cavani, F. Trifiro, A. Vaccari, Catal. Today 11 (1991) 173.
[9] R. Oesten, H. Böhm, Solid State Ionics 62 (1993) 199.
[10] V.R.L. Constantino, T.J. Pinnavaia, Inorg. Chem. 34 (1995) 883.
[11] A.I. Khan, D. O' Hare, J. Mater. Chem. 12 (2002) 3191.
[12] S.P. Newman, W. Jones, New J. Chem. (1998) 105.
[13] S. Carlino, Solid State Ionics 98 (1997) 73.
[14] R.L. Goswamee, P. Sengupta, K.G. Bhattacharyya, D.K. Dutta, Appl. Clay Sci. 13 (1998) 21.
[15] B. Houri, A. Legrouri, A. Barroug, C. Forano, J.P. Besse, Collect. Czech. Chem. Commun. 63 (1998) 732.
[16] R.K. Allada, A. Navrotsky, H.T. Berbeco, W.H. Casey, Science 296 (2002) 721.
[17] E.L. Crepaldi, P.C. Pavan, J.B. Valim, J. Mater. Chem. 10 (2000) 1337.
[18] I. Crepani, M. Berrettoni, B. Ballarin, M. Giorgetti, E. Scavetta, D. Tonelli, Solid State Ionics 168 (2004) 167.
[19] F. Kooli, W. Jones, V. Rives, M.A. Ullibarri, J. Mater. Sci. Lett. 16 (1997) 27.
[20] T. Hibino, A. Tsunashima, Chem. Mater. 9 (1997) 2082.
[21] E.M. Serwica, P. Nowak, K. Bahranowski, W. Jones, F. Kooli, J. Mater. Chem. 7 (1997) 1937.
[22] S.V. Prasanna, P.V. Kamath, unpublished work.
[23] A.V. Radha, P.V. Kamath, C. Shivakumara, Solid State Sci. 7 (2005) 1180.
[24] J.W. Boclair, P.S. Braterman, Chem. Mater. 11 (1999) 298.
[25] W.T. Reichle, Solid State Ionics 22 (1986) 135.
[26] G. Brauer (Ed.), Handbook of Preparative Inorganic Chemistry, vol. 2, Academic Press, New York, 1965, p. 1549.
[27] M.M.J. Treacy, M.W. Deem, J.M. Newsam, DIFFaX, Version 1.807.
[28] G.S. Thomas, M. Rajamathi, P.V. Kamath, Clays Clay Miner. 52 (2004) 693.
[29] T.N. Ramesh, M. Rajamathi, P.V. Kamath, Solid State Sci. 5 (2003) 751.
[30] H.F.W. Taylor, Mineral. Mag. 39 (1973) 377.
[31] Y.G. Andreev, T. Lundstrom, J. Appl. Crystallogr. 27 (1994) 767.
[32] K. El-Malki, A. de Roy, J.P. Besse, Eur. J. Solid State Inorg. Chem. 26 (1989) 339.
[33] S.D. Ross, Inorganic Infrared and Raman Spectra, McGraw–Hill, London, 1972.
[34] F. Malherbe, J.P. Besse, J. Solid State Chem. 155 (2000) 332.
[35] J. Chevanas, J.C. Joubert, J.J. Capponi, M. Marezio, J. Solid State Chem. 6 (1973) 1.
[36] A.S. Bookin, V.A. Drits, Clays Clay Miner. 41 (1993) 551.
[37] N.N. Das, J. Konar, M.K. Mohanta, S.C. Srivastava, J. Colloid Interface Sci. 270 (2004) 1.
[38] M. Jobbagy, A.E. Regazzoni, J. Phys. Chem. B 109 (2005) 389.